24th International Liquid Crystal Conference Mainz, August 19th - 24th, 2012

Scientific Program

Monday, 20.08.2012

3. Pattern formation and dynamics (a)	*Convention Center Mainz* *Lecture Hall A*
14:00 - 14:30	**Invited Lecture:** Nemato-Microfluidics: Interplay between Flow, Confinement and Surface Anchoring on a Microfluidic Platform (Abstract)
	Sengupta, A., Göttingen/D, Bahr, C., Goettingen/D, Herminghaus, S., Goettingen/D
14:30 - 14:45	Active and passive nematic flow in micro-channels (Abstract)
	Ravnik, M., Ljubljana/SLO, Yeomans, J. M., Oxford/GB
14:45 - 15:00	Single molecule diffusion in molecularly thin free-standing liquid crystal films (Abstract)
	Schulz, B., Göttingen/D, Bahr, C., Göttingen/D
15:30 - 15:45	Liquid crystals cosmology (Abstract)
	Simões, M., Londrina/BR
15:45 - 16:00	Periodic lattices of frustrated focal conic defect domains in smectic liquid crystal films (Abstract)
	Zappone, B., Rende/I, Meyer, C., Amiens/F, Bruno, L., Rende/I, Lacaze, E., Paris/F
16:00 - 16:30	**Invited Lecture:** Competition between Electric Field Induced Equilibrium and Dissipative Patterns at Low Frequency Driving in Nematics (Abstract)
	Eber, N., Budapest/H, Palomares, L. O., Budapest/H, Salamon, P., Budapest/H, Krekhov, A., Budapest/H, Buka, A., Budapest/H
16:30 - 16:45	Flexoelectricity and Pattern Formation in Nematic Liquid Crystals (Abstract)
	Krekhov, A., Bayreuth/D, Pesch, W., Bayreuth/D, Buka, A., Budapest/H
16:45 - 17:00	Electric-field induced pattern formation, microscopic dynamics and criticality in suspensions of charged fibrous viruses (fd) (Abstract)
	Kang, K., Juelich/D, Dhont, J. K. G., Juelich/D

Competition between Electric Field Induced Equilibrium and Dissipative Patterns at Low Frequency Driving in Nematics.

N. Éber,[1,*] L.O. Palomares,[1] P. Salamon, [1] A. Krekhov,[2] and Á. Buka [1]

[1]*Institute for Solid State Physics and Optics, Wigner Research Centre for Physics,*
Hungarian Academy of Sciences, Budapest, Hungary
[2]*Institute of Physics, University of Bayreuth, Bayreuth, Germany*

Applying an electric field onto a planarly oriented thin layer of a nematic liquid crystal often leads to the appearance of spatially periodic structures – stripe patterns. Electroconvection (EC) rolls [1,2] and flexoelectric domains (FD) [3] are long known examples of such patterns, representing different driving mechanisms.

According to the simple theoretical model by Bobylev and Pikin [3,4] and its recent generalization for anisotropic elasticity and AC driving by Krekhov et al. [5] the FD pattern corresponds to a spatially periodic equilibrium director deformation caused by flexoelectricity. FD have been observed by polarizing microscopy in a few nematics; manifesting itself as a sequence of dark and bright stripes running parallel to the initial director. EC is a more complex phenomenon – a non-equilibrium, dissipative response to the excitation by an applied voltage. It involves besides director modulation also charge separation and vortex flow. EC patterns occur more frequently than FD and exhibit a wide morphological richness (in the magnitude and direction of the wave vector $\mathbf{q}$) [2]. Here we limit ourselves to standard EC which arises in nematics with a negative anisotropy of the dielectric permittivity ($\varepsilon_a < 0$) and a positive electrical conductivity anisotropy ($\sigma_a > 0$). Then EC rolls look similar to FD, however, they are running normal or obliquely to the initial director. This type of pattern formation is well understood via the Carr-Helfrich feedback mechanism [1]; the precise theoretical description combines the equations of electro- and nematohydrodynamics known as the standard model (SM) of EC [6] which has recently been extended by the inclusion of flexoelectric effects [7].

Flexoelectric domains and electroconvection have usually been studied in different frequency ranges: FD are typically seen at DC applied voltages while EC rolls are mostly investigated with AC driving of $f > 10$ Hz where the period $T = 1/f$ of the voltage is short compared to the characteristic relaxation time τ of the pattern (which scales with the director relaxation time [8]). This latter means that several periods are required for the pattern to evolve or decay. It has been proved both experimentally and theoretically that in this frequency range the two regimes of standard EC – the conductive and the dielectric ones – differ in their temporal behaviour within a driving period: in the conductive regime the director tilt is stationary resulting in a nearly constant (within T) pattern contrast while in the dielectric regime the director tilt oscillates with f, hence the system goes through the initial state and thus the contrast falls down to zero in each half period.

The other limit ($T \gg \tau$) has not attracted much attention until recently when May at el. [9] reported a crossover between FD and standard dielectric EC rolls at ultra-low ($f < 1$ Hz) driving frequencies. Moreover, they observed that both patterns exist only as flashes in part of the half period $T/2$.

Below we will show that this behaviour is more general: standard conductive EC rolls also exhibit a flashing character and we found a crossover to FD at ultra-low frequency driving. We will also demonstrate that these features are in good agreement with the theoretical predictions, i.e with the results of the linear stability analysis of the SM extended by flexoelectricity [5,7], which is able to describe both EC patterns and also the FD by a subset of the equations.

---

*presenting author; E-mail:eber.nandor@wigner.mta.hu

Experiments have been carried out on the nematic mixture Phase 5 (Merck) at the temperature of $T = 30 \pm 0.05$ ^{o}C using planar cells of $d = 11.3$ μm thickness. This compound exhibits FD at DC driving and standard conductive EC rolls at AC voltages up to a frequency of $f \approx 230$ Hz where a crossover to dielectric EC rolls occurs. The voltage-induced patterns were observed by a polarizing microscope at white light illumination using the shadowgraph (single polarizer) technique. Sequences of snapshot images were recorded by an attached high speed camera at variable (≤ 2000 frames/s) rate with a spatial resolution of 512*512 pixels at 256 grey levels. The start of recording was synchronized with the negative zero crossing of the applied sinusoidal voltage allowing to monitor the temporal variations within the driving period in 20 - 4000 time instants (depending on f). For a quantitative analysis the image contrast $C(t)$ was defined as the mean square deviation of the intensity, $C = \langle(I_{ij} - \langle I_{ij}\rangle)^2\rangle$ (here I_{ij} is a pixel's intensity and $\langle\rangle$ denotes averaging over the whole image). The contrast $C_0 \neq 0$ obtained for the initial undistorted state at no applied voltage (originating e.g. from from thermal fluctuations) was regarded as a background value to be subtracted from $C(t)$.
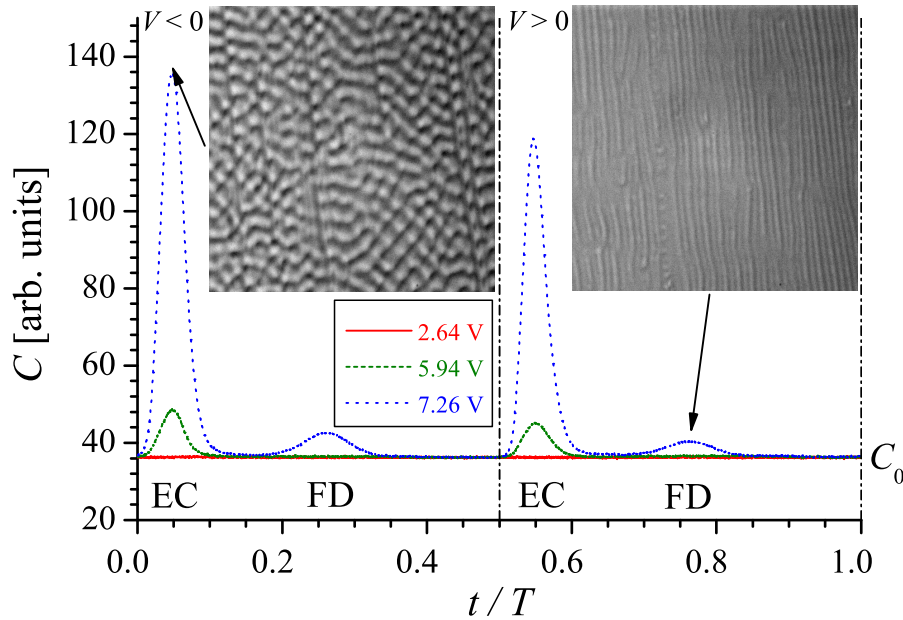

Figure 1: Temporal evolution of the pattern contrast $C(t)$ for $f = 0.03$ Hz within a driving period T at $V < V_{EC}$ (solid red line), at $V_{EC} < V < V_{FD}$ (dashed green line) and at $V_{FD} < V$ (dotted blue line). C_0 is the background contrast of the initial state. The two snapshots taken at the maxima of the contrast spikes represent the different pattern morphologies: overlapping conductive oblique rolls (EC, left) and flexoelectric domains (FD, right).

The ultra-low frequency behaviour of the sample was tested at $f = 0.03$ Hz at increasing voltages. Figure 1 shows the time evolution of the contrast $C(t)$ for one driving period T at selected voltages. It can be seen that at a low applied voltage the background subtracted contrast is zero, hence no pattern is there. If the voltage exceeds a threshold rms value V_{EC} a spike appears in $C(t)$ around $t_{EC} \approx 0.05T + nT/2$ indicating that an EC pattern evolves which could be identified as (superposed) conductive oblique rolls. When the applied voltage exceeds a (higher) second threshold V_{FD} another spike emerges in the contrast around $t_{FD} \approx 0.26T + nT/2$ corresponding to the parallel stripes of FD. In the formulae above n is an integer indicating that the scenarios repeat themselves in time with the periodicity of the half period. It is evident from Fig. 1 that both the EC and FD patterns exist only in a small part of the half period; moreover

the time windows of their existence is time separated.

On the one hand, the flashing character of the patterns shown above might have been anticipated, in view of the $T \gg \tau$ condition meaning that there is enough time for the pattern to evolve and decay within a half period. Then one might naively expect that the existence window of the pattern should be centred roughly around the time instants of the voltage maxima ($T/4 + nT/2$). This seems to fulfil for FD but does not hold for EC. On the other hand, while the flashing character of the dielectric rolls [9] were not so surprising due to the oscillation of the director, it was quite unexpected for the conductive EC rolls since they have been known to be characterized by a stationary director modulation at usual ($f > 10$ Hz) frequencies.
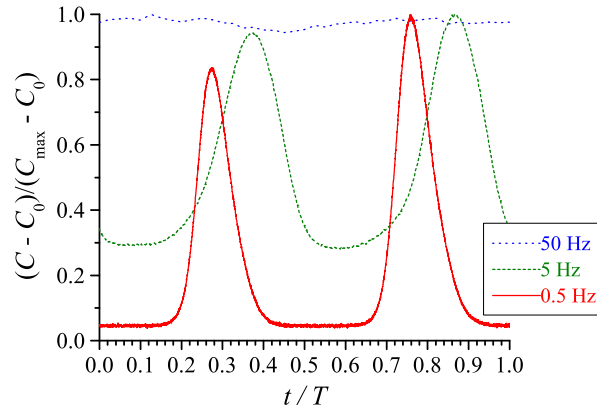

Figure 2: The measured temporal evolution of the background subtracted normalized contrast within one period at different driving frequencies.

In order to find out how the stationary conductive roll pattern transforms into a flashing one we measured the temporal evolution within the driving period in a wide (0.01 – 100 Hz) frequency range. Figure 2 presents the background subtracted normalized contrast $\gamma(t) = (C(t) - C_0)/(C_{max} - C_0)$ for one period for three selected frequencies (here C_{max} stands for the maximum of $C(t)$ within the period). As can be seen, at high f (50 Hz) the contrast is almost constant as is expected for a stationary pattern. Reducing the frequency (5 Hz) the contrast becomes strongly modulated, but its minimum value C_{min} is much above C_0, i.e. the pattern is still present all the time. At low frequency (0.5 Hz), however, $C_{min} = C_0$ indicates that the pattern decays fully within a half period and then it develops again. This process is seen in more detail in Fig. 3 which depicts the frequency dependence of the background subtracted normalized contrast minima $\gamma_{min} = (C_{min} - C_0)/(C_{max} - C_0)$ by solid symbols. The transition from the stationary pattern ($\gamma_{min} \approx 1$) to the flashing one ($\gamma_{min} \approx 0$) occurs in the frequency range of 1 Hz $\leq f \leq$ 30 Hz. We note here that the characteristic frequency τ_d^{-1} calculated from the director relaxation time for the tested sample is about 7 Hz which falls in the middle of this transition f range.

In order to compare the obtained results with the theoretical predictions of the extended SM [5,7] the temporal evolution of the director component normal to the substrates ($n_z(t)$) was calculated numerically by a linear stability analysis for the midplane of the cell (where the director tilt is the largest). Though the spatial modulation of n_z is responsible for the optical pattern observed, the relation between the contrast C and n_z is by far not trivial and may be different (quadratic or linear [9]) for patterns of different origin (like EC and FD). Therefore $C(t)$ has not been calculated, rather the experimental $C(t)$ was compared with the calculated $n_z(t)$ ($C(t)$ and $n_z(t)$ are expected to take their maximum values in the same time instants). In the calculations the known material parameter set of Phase 5 [7] was used with the conductivity adjusted
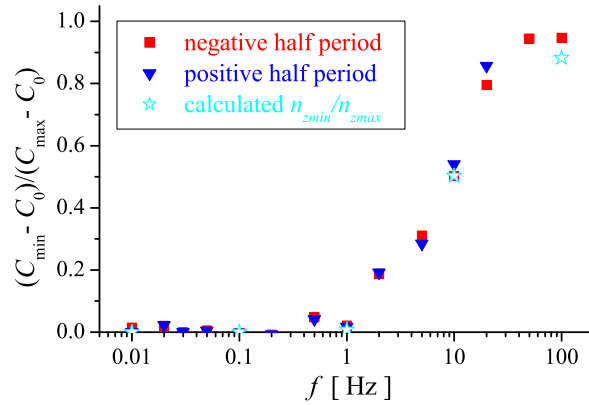
Figure 3: The measured frequency dependence of the background subtracted normalized contrast minima for conductive EC rolls.

to the conductive - dielectric crossover frequency and the flexocoefficients estimated from the wavelength of the FD pattern. The calculations have confirmed that $n_z(t)$ behaves similarly to $\gamma(t)$ shown in Fig. 2: in the conductive EC pattern it has a $2f$ modulation, the amplitude of which is negligible at high f (stationary pattern), but grows rapidly when f is reduced and finally at ultra-low frequencies $n_z(t)$ takes the spiky character, just as was found for $\gamma(t)$. The calculated n_{zmin}/n_{zmax} is also plotted in Fig. 3 by open symbols; the matching with $\gamma_{min}(f)$ is quite convincing.
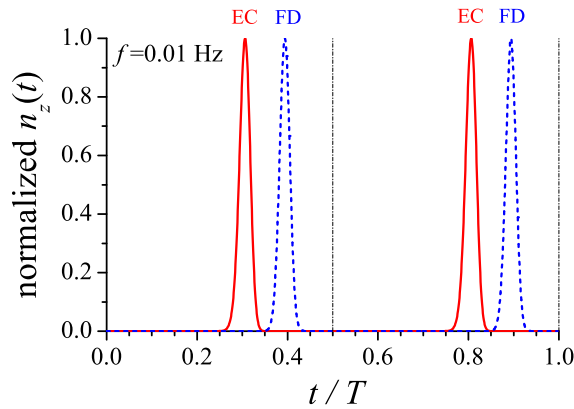

Figure 4: Temporal evolution of the calculated director component n_z for EC and FD in the midplane of the sample within one period at $f = 0.01$ Hz.

Using the same equations but with no flow and no electrical conductivity ($\mathbf{v} = 0$ and $\sigma = 0$) the director field of FD could also be calculated. Figure 4 shows the temporal evolution of the normalized $n_z(t)$ within a driving period calculated for the ultra-low frequency of $f = 0.01$ Hz, both for FD and conductive EC. It is immediately perceptible that there is an excellent qualitative agreement with the experimental findings in Fig. 1: for both patterns $n_z(t)$ exhibits spikes similar to those of $C(t)$ and the deformation in the two patterns occurs in different time windows. We note here that the latter statement holds for very low f only; even for slightly higher frequencies (e.g. for $f = 0.1$ Hz) the calculated $n_z(t)$ of EC and FD overlap in time and experimentally the EC pattern does not decay before FD emerge; rather a rotation of the wave
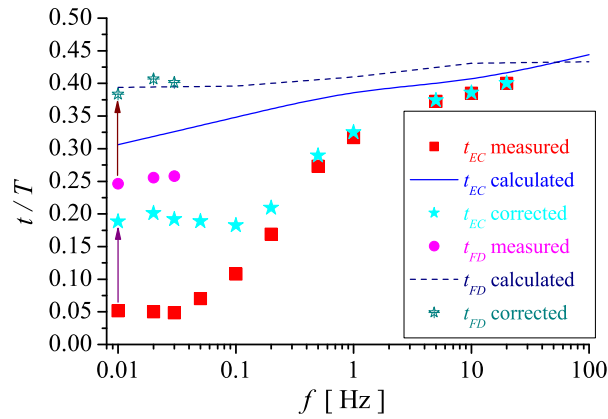
vector could only be observed.

Figure 5: Frequency dependence of the measured (solid symbols) and calculated (curves) location of contrast maxima for the EC and FD patterns. Star symbols indicate corrected values.

The time instants when the measured $C(t)$ or the calculated $n_z(t)$ have their maxima within a driving period, depends on the frequency. Figure 5 exhibits their locations for the EC rolls (t_{EC}/T) as well as for the FD pattern (t_{FD}/T). It can be seen that the frequency dependence of t_{EC} is stronger than that of t_{FD}. Moreover, the experimental values are considerably closer to zero than the theoretical ones and the experimental $t_{FD} - t_{EC}$ is also larger than expected.

A possible reason for this quantitative mismatch may come from the fact that in the theoretical description $V = V_{LC}$ is always the voltage applied directly onto the liquid crystal layer, while experimentally V is the voltage applied to the cell. The planar orientation of the cell is provided by a thin polyimide (PI) layer which is a better insulator than the liquid crystal (LC) itself. As a consequence the cell may be represented by an electrical equivalent circuit consisting of two parallel resistor (R) – condenser (C) circuits (one for the PI and another for the LC) connected in series; hence actually $V = V_{PI} + V_{LC}$. At the usual high ($f > 10$ Hz) frequencies the voltage attenuation is mostly capacitive. Since the thickness of the PI layer is very small, its capacitance is much larger than that of the LC and therefore V_{PI} is negligibly small. At ultra-low frequencies, however, the attenuation becomes mostly resistive; V_{PI} and V_{LC} may be of the same order of magnitude and, in general, both are phase shifted with respect to the applied voltage V.

Unfortunately V_{LC} and hence its phase shift with respect to the applied voltage is not directly measurable. Indirectly one can get information on that by monitoring the frequency dependent phase shift ϕ of the current flowing through the cell with respect to V. If the time constants RC of the PI and the LC layers are different (which is the typical case), ϕ exhibits a non-monotonic frequency dependence, which has actually been observed in the experiment as shown if Fig. 6. A fitting of experimental data with ϕ calculated from the equivalent circuit yields an estimation for the R and C values of PI and LC. Using those values the phase shift $\varphi(f)$ between V_{LC} and V could also been calculated. The locations of the spike maxima shown in Fig. 5 were obtained with respect the zero crossing of the applied voltage V. Now using $\varphi(f)$ these values can be corrected to obtain the spike locations with respect to the voltage V_{LC} on the LC layer (the star symbols in Fig.5). It can be seen that the correction is negligible at high f, but becomes crucial at the ultra-low frequency range (see the arrows in Fig. 5). The corrected t_{FD} values are in excellent agreement with the theoretical expectations. The mismatch in t_{EC} is also reduced considerably. The remaining difference may be owing to ionic effects, which are not included in the extended SM of EC, though
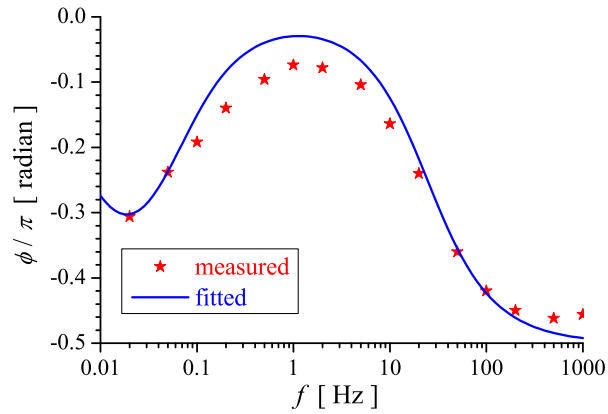
Figure 6: Frequency dependence of the phase ϕ of the current with respect to the applied voltage. Stars represent measured values, the solid line is a fit using the electrical equivalent circuit.

becoming more relevant at ultra-low frequencies than at high f. An experimental indication of these ionic effects is the distortion of the current waveform (a peak superposed on the sine at the zero crossing of V) appearing below $f = 1$ Hz.

Summarizing, we have investigated the temporal evolution of electric field induced patterns in a wide (0.01 - 100 Hz) frequency range. At ultra-low f we have seen a crossover between two types of patterns: the non-equilibrium dissipative conductive electroconvection rolls and the equilibrium deformation called flexoelectric domains. We have proved experimentally as well as by theoretical calculations that at such ultra-low frequencies both patterns possess a flashing character, i.e. the patterns exist only in narrow time windows within the driving period. The electroconvection rolls and the flexodomains are well separated in time as well as in the **q**-space; the transition from one to the other occurs repetitively in each half period of the driving. We have explored how the high f stationary conductive EC rolls transform into the ultra-low f flashing pattern. We have measured and calculated where the flashing patterns are located within the driving period. We have proved by current measurements that owing to the polyimide orienting layers the actual voltage on the liquid crystal layers differs from the applied voltage due to an internal voltage attenuation and phase shift, which has to be taken into account when comparing experimental data with theoretical predictions.

References:

[1] L. Kramer, and W. Pesch, *Electrohydrodynamic instabilities in nematic liquid crystals*, In eds. A. Buka, and L. Kramer, *Pattern Formation in Liquid Crystals*, Springer, New York, 1996, p. 221.

[2] Á. Buka, N. Éber, W. Pesch, and L. Kramer, *Convective patterns in liquid crystals driven by electric field. An overview of the onset behaviour*, In Eds. A.A. Golovin, A.A. Nepomnyashchy. *Self-Assembly, Pattern Formation and Growth Phenomena in Nano-Systems*, NATO Science Series II, Mathematica, Physics and Chemistry, Vol. **218**, Springer, Dordrecht, 2006, p. 55.

[3] S. A. Pikin, *Structural Transformations in Liquid Crystals*, (Gordon and Breach Science Publishers, 1991).

[4] Yu. P. Bobylev, and S. A. Pikin, *Threshold piezoelectric instability in a liquid crystal*, Sov. Phys. JETP **45**, 195 (1977).

[5] A. Krekhov, W. Pesch, and Á. Buka, *Flexoelectricity and pattern formation in nematic liquid crystals*, Phys. Rev. E **83**, 051706 (2011).

[6] E. Bodenschatz, W. Zimmermann, and L. Kramer, *On electrically driven pattern forming instabilities in planar nematics*, J. Phys. (France) **49**, 1875 (1988).

[7] A. Krekhov, W. Pesch, N. Éber, T. Tóth-Katona, and Á. Buka, *Nonstandard electroconvection and flexoelectricity in nematic liquid crystals*, Phys. Rev. E **77**, 021705 (2008).

[8] N. Éber, S. A. Rozanski, S. Németh, Á. Buka, W. Pesch, and L. Kramer, *Decay of spatially periodic patterns in a nematic liquid crystal*, Phys. Rev. E **70**, 061706 (2004).

[9] M. May, W. Schöpf, I. Rehberg, A. Krekhov, and Á. Buka, *Transition from longitudinal to transversal patterns in an anisotropic system*. Phys. Rev. E **78**, 046215 (2008).